ARTICLE

Check for updates

A loss of function variant in *AGPAT3* underlies intellectual disability and retinitis pigmentosa (IDRP) syndrome

Madiha Amin Malik[1,2], Muhammad Arif Nadeem Saqib[3], Edwin Mientjes[2], Anushree Acharya[4], Muhammad Rizwan Alam[1], Ilse Wallaard[2], Isabelle Schrauwen[4], Michael J. Bamshad[5,6], Regie Lyn P. Santos-Cortez[7], Ype Elgersma[2], Suzanne M. Leal[4,8]✉ and Muhammad Ansar[1]✉

Intellectual disability (ID) and retinal dystrophy (RD) are the frequently found features of multiple syndromes involving additional systemic manifestations. Here, we studied a family with four members presenting severe ID and retinitis pigmentosa (RP). Using genome wide genotyping and exome sequencing, we identified a nonsense variant c.747 C > A (p.Tyr249Ter) in exon 7 of *AGPAT3* which co-segregates with the disease phenotype. Western blot analysis of overexpressed WT and mutant AGPAT3 in HEK293T cells showed the absence of AGPAT3, suggesting instability of the truncated protein. Knockdown of *Agpat3* in the embryonic mouse brain caused marked deficits in neuronal migration, strongly suggesting that reduced expression of AGPAT3 affects neuronal function. Altogether, our data indicates that *AGPAT3* activity is essential for neuronal functioning and loss of its activity probably causes intellectual disability and retinitis pigmentosa (IDRP) syndrome.

European Journal of Human Genetics (2023) 31:1447–1454; https://doi.org/10.1038/s41431-023-01475-w

INTRODUCTION

Intellectual disability (ID) is generally characterized by the presence of low cognitive function (IQ score <70) and inability to perform certain social and adaptive tasks. In a number of syndromes, that include Bardet-Biedl syndrome (BBS) [1, 2], Joubert syndrome (JS) [3], Cohen syndrome (CS) [4], Senior-Löken syndrome (SLS) [5], and Meckel Gruber Syndrome (MKS) [6] patients display both ID and retinal dystrophies (RDs). Most of these syndromes are clinically and genetically heterogeneous.

In addition to these well-established pleiotropic syndromes, variants in a few additional genes are known to be associated with both ID and retinitis pigmentosa (RP), the most common form of RD, along with additional variable clinical features [7]. For instance, mutations in *SCAPER* were initially reported to cause RP, ID and attention deficit hyperactivity disorder (ADHD) [8], but subsequent studies expanded the phenotypic spectrum associated with this gene [9] and argued its involvement in Bardet-Biedl syndrome [10]. Similarly, biallelic mutations in the *RCBTB1* gene have been identified in patients presenting mild ID and RP along with additional features that include goitre and primary ovarian insufficiency [11]. Another syndrome (SHRF; MIM 617763) that include RP, brachydactyly, myopia, short stature, mild ID, hypothyroidism, facial dysmorphism and progressive hearing loss is due to variants in *EXOSC2* [12]. These examples demonstrate the involvement of ID and RP phenotypes in multiple syndromes, although patients presented in the above studies also exhibited additional clinical features.

Phosphatidic acid (PA) is used as a precursor for the synthesis of glycerophospholipids (GPLs) like phosphatidyl choline, phosphatidyl ethanolamine, phosphatidyl serine and phosphatidyl inositol. GPLs are important components of membranous structures in cells and can also act as signaling molecules [13–15]. PA is synthesized by the esterification reaction of fatty acid at sn-2 position of lysophosphatidic acid (LPA) and this reaction is catalyzed by a family of enzymes known as 1-acylglycerol-3 phosphate-O-acyltransferases (AGPAT). There are eleven known isoforms expressed by the AGPAT gene-family [16]. These isoforms are tissue and substrate specific [17] and loss of any isoform is not compensated by other isoforms [16]. One of the isoforms, 1-acylglycerol-3-phosphate-O-acyltransferase3 (*AGPAT3*), also known as lysophosphatidic acid acyltransferase 3 (*LPAAT3*), is localized in the endoplasmic reticulum and golgi complex. It is involved in the conversion of LPA into PA and regulates the structure, trafficking and tubule formation of golgi complex by altering the composition of phospholipids and lysophospholipids [18]. Human *AGPAT3* has four motifs (I-IV) which are involved in catalysis and substrate recognition [19]. These motifs are conserved among the AGPAT family and site-directed mutagenesis of different residues located within the *AGPAT1* motifs, revealed their importance in the catalysis [20]. A cell line-based study (on Hela cells) confirmed AGPAT3 localization in the endoplasmic reticulum (ER) and golgi, and its knockdown by siRNA resulted in Golgi fragmentation [18]. This work provided initial evidence on the role of AGPAT3 in the

[1]Department of Biochemistry, Faculty of Biological Sciences, Quaid-I-Azam University, Islamabad 45320, Pakistan. [2]Department of Neuroscience, Erasmus University Medical Center, Rotterdam, The Netherlands. [3]Department of Medical Laboratory Technology, National Skills University, Islamabad 44000, Pakistan. [4]Center for Statistical Genetics, Gertrude H. Sergievsky Center, and the Department of Neurology, Columbia University Medical Center, New York, NY, USA. [5]Department of Genome Sciences, University of Washington, William H. Foege Hall, 3720 15th Ave. NE, Seattle, WA 98195, USA. [6]Department of Pediatrics, University of Washington, Seattle, WA, USA. [7]Department of Otolaryngology-Head and Neck Surgery, School of Medicine, University of Colorado Anschutz Medical Campus (CU-AMC), 12700 E. 19th Ave, Aurora, CO 80045, USA. [8]Taub Institute for Alzheimer's Disease and the Aging Brain, Columbia University Medical Center, New York, NY, USA. ✉email: sml3@cumc.columbia.edu; ansar@qau.edu.pk

Received: 13 June 2023 Revised: 17 August 2023 Accepted: 27 September 2023
Published online: 11 October 2023

regulation of Golgi tubule formation, trafficking, and structure by altering phospholipids and lysophospholipids. Furthermore, *Agpat3* knockout mice exhibit impaired vision due to abnormalities in the retinal layers [21] and male infertility due to abnormal sperm morphology [22]. The retina of *Agpat3* knockout mice lack docosahexaenoic acid containing phospholipids (PL-DHA), and this loss alters disc morphology, reduces the length of the outer segment and decreases the thickness of outer nuclear layers [21]. However, none of the earlier studies reported cognitive impairment in *Agpat3* knockout mice.

In this study, we performed genetic analysis on a consanguineous Pakistani family presenting IDRP syndrome and identified a nonsense variant in *AGPAT3*. We also showed that *AGPAT3* knockdown in the developing mouse brain affects neuronal migration of the targeted cells to the outer cortical layers.

MATERIALS AND METHODS

Family recruitment and clinical evaluation

Family MR23 was recruited from the interior region of the Sindh province of Pakistan and the pedigree was drawn (Fig. 1a) based on the information collected from healthy family members. This family has four individuals suffering from IDRP syndrome inherited in an autosomal recessive manner. Blood samples of available affected and unaffected individuals were collected, and the genomic DNA was extracted. Clinical diagnosis was done based on apparent clinical symptoms, fundoscopy, optical coherence tomography (OCT), cranial tomography (CT) scan, magnetic resonance imaging (MRI), liver function tests (LFTs) and renal function tests (RFTs). Consent in writing was obtained from healthy individuals and guardians of individuals with ID. Ethical approval for this research work was obtained from the Bio-Ethics Committee (BEC-562) of the Faculty of Biological Sciences, Quaid-I-Azam University, Islamabad, Pakistan and Institutional Review Board (IRB), at Columbia University (IRB-AAAS3433), USA. Animal experiments were performed in accordance with European Commission Council Directive 2010/63/EU (CCD approval AVD101002017893) at Erasmus Medical Center, Rotterdam, Netherlands.

Homozygosity mapping

DNA samples of three affected (V-2, V-3 and V-5) and three normal (III-3, V-4 and V-6) members underwent genome wide mapping using Infinium® Human Core Exome Bead Chip, ~550 K Array, (Illumina, USA) and data were analyzed using Homozygosity mapper [23] to identify the homozygous intervals shared by the three affected members. Each potential homozygous region was explored using Gene Distiller to check the presence of genes expressed in the brain or associated with already reported genes linked with ID and RP. Copy number variations (CNVs) were also analyzed to exclude the presence of numerical chromosomal changes or large deletions.

Whole exome sequencing

Exome sequencing (WES) was performed using a DNA sample obtained from affected individual V-3. Roche NimbleGen SeqCap EZ Human Exome Library v.2.0 was used to perform sequence capture to target ~37 MB coding sequence. Sequencing of the sample was performed on Illumina Hiseq platform with the average sequencing depth of 60x of the targeted region. Burrows–Wheeler Aligner was used to align fastq files to the reference human genome sequence (GRCh37/hg19) and Genome Analysis Toolkit was used to realign indel regions, variant identification and calling and recalibration of base quality as performed previously [24]. Annotation of variant call file was performed using wANNOVAR.

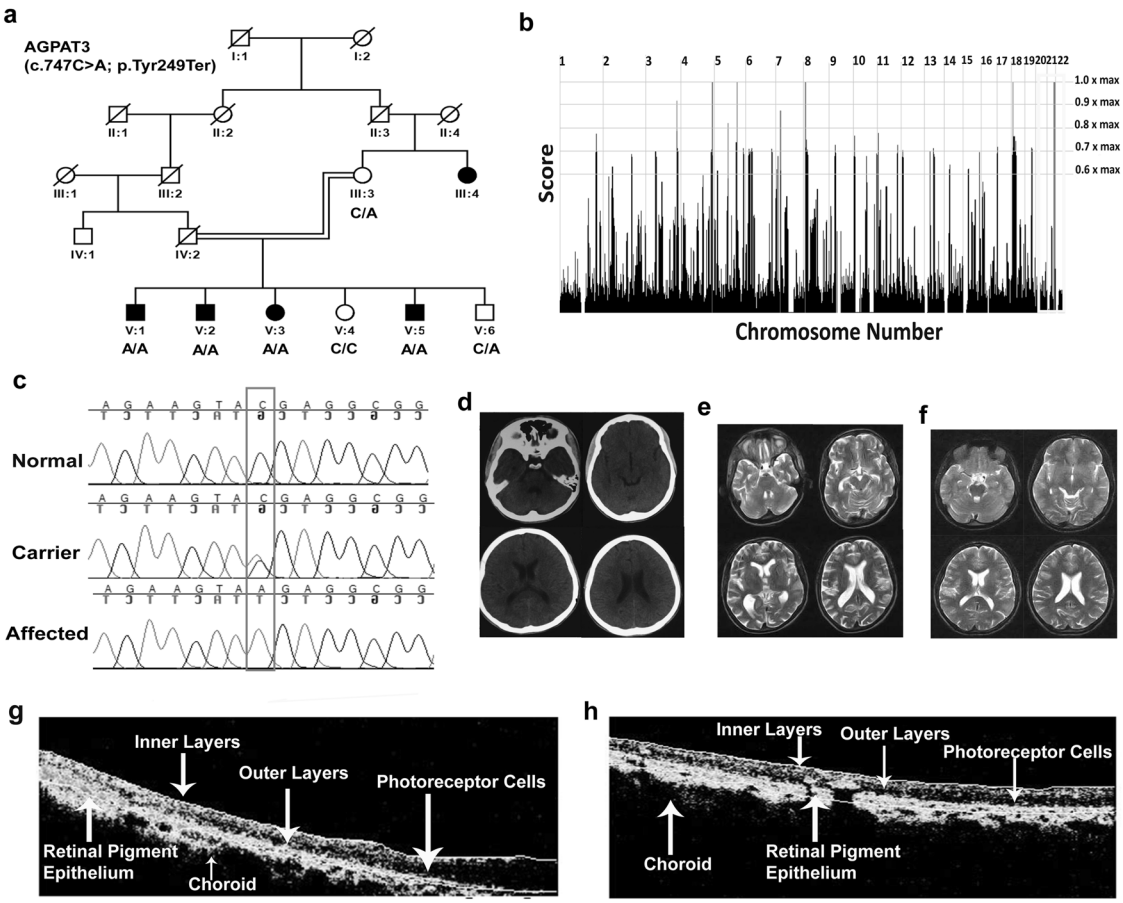

Fig. 1 Pedigree and clinical information of family with IRDP syndrome. a Five generation pedigree and haplotype of the family with IDRP syndrome. **b** Homozygosity mapper output showing homozygous by descent (HBD) regions. Red peaks represent homozygous regions detected across the chromosome. **c** Co-segregation of variant c.747 C > A with disease phenotype. **d** CT scan of V-5 individual and (**e**) MRI of individual V-1 and (**f**) V-5 generally show normal features. **g**, **h** OCT of right eye of individual V-5 showed poor retinal architecture. The retina appears thinned and without clear outer segment (Photoreceptor cells).

Exome data was analyzed to identify coding and splice site variants which had <0.01 minor allele frequency (MAF) in genome aggregation database (gnomAD) and were absent in dbSNP. Pathogenicity of the identified variants was predicted by Provean, Mutation Taster, Polyphen2, FATHMM and SIFT. Finally, based on the autosomal recessive inheritance of IDRP syndrome, potential homozygous variants were selected for segregation analysis in remaining family members for which a DNA sample was available.

Segregation analysis

Co-segregation of c.747 C > A variant was confirmed using forward 5′-CTTTTCCCTCTGGCAGTGAC-3′ and reverse 5′-GTCTCCATGTCCTCTCCGTG-3′, primers designed to flank regions of exon 7 of *AGPAT3* (NM_020132). DNA samples of all available members of the MR23 family were used to amplify exon 7 and the amplified products were purified using ExoSAP-IT (Affymetrix, Cleveland, OH, USA) and subjected to sequencing using BigDye Terminator v3.1 Cycle Sequencing Kit (Life Technologies, Carlsbad, CA, USA). The sequence data was analyzed with Sequencher 5.4.6 (Gene Codes Corporation, Ann Arbor, MI, USA).

Plasmid constructs and transfection

The complementary DNA (cDNA) from human AGPAT3 (NM_020132) was synthesized from human brain total RNA (iScript™ cDNA synthesis kit, Bio-Rad) and amplified by PCR (Phusion high fidelity kit, Thermo Fisher Scientific, USA) using forward primer 5′-GTCGAGAATTCTAAGGCGCGCCACC ATGGGTAAGCCTATCCCTAACCCTCTCCTCGGTCTCGATTCTACGGGTGCTGGC CTGCTGGCCTTCCTGAAG-3′ (containing V5 tag) and reverse primer 5′-GTCGACTTAATTAATTATTCCTTTTTCTTAAACTC-3′, cut with Asc-I and Pac-I and inserted into the multiple cloning site downstream of the CAGG promoter of our dual promoter expression plasmid. The plasmid also contains a pGK-*tdTomato* reporter. The variant (c.747 C > A) was introduced in the cloned *AGPAT3* cDNA by site-directed mutagenesis (Phusion Thermo Fisher Scientific, USA) with 5′-TCCTCTACGGGAAGAAGTAAGAGGCGGACA TGTGCGTGAG-3′ and 5′-CTCACGCACATGTCCGCCTCTTACTTCTTCCCGTAGA GGA-3′ primers. The same vector without *AGPAT3* cDNA was used as a control for in vitro experiments. All constructs were verified by Sanger sequencing (Macrogen, Europe).

Both mutant and wild type constructs were expressed in HEK-293T cells cultured in DMEM containing 10% fetal calf serum (FCS) and 1% penicillin/streptomycin in 6-well plates. Cells were transfected with control vector, $AGPAT3^{WT}$ and $AGPAT3^{p.Tyr249Ter}$ (3 µg per well) in triplicate and transfection was performed by using polyethylenimine (PEI, Polysciences) according to the manufacturer protocol. Twenty-four hours after transfection, the medium was refreshed to reduce PEI toxicity and cells were harvested after 48 h for western blot.

The shRNA constructs for in vivo experiments were purchased from MISSION shRNA library for mouse genomes of Sigma Life Sciences and The RNAi Consortium (TRC). Four different shRNA expressing plasmids (GCTGTGATTGAACACCCATAA, CTAGAGATCGTATTCTGCAAA, GCTATGGCAA CCAAGAGCTTA and GATCGTATTCTGCAAACGGAA) were used to knock down the expression of *AGPAT3* in the brain of mouse embryos. As a control, the MISSION non-targeting shRNA control vector (CAACAAGATG AAGAGCAGGAA) was used.

Western blotting

HEK cells were homogenized in 1X Laemmli buffer (0.2 M Tris–HCl [pH 6.8], 10% glycerol, 1 mM EDTA, 0.004% bromophenol blue, 1.5% sodium dodecyl sulfate [SDS]) and protease inhibitor (Sigma) by sonication. The protein quantity was determined by BCA protein assay (Pierce Thermo Fisher Scientific, USA) and concentration was adjusted to 1ug/ul. For Western blots, 20ug of lysate was separated on SDS-PAGE (4–12% Criterion XT Bis-Tris gel, Bio-Rad) and transferred to a nitrocellulose membrane using the turbo blot (Bio-Rad). Blots were blocked in 4% milk in TBS (10 mM Tris–HCl at pH 8.0, 150 mM NaCl) for half an hour and then probed with primary antibodies against V5 tag of *AGPAT3* (mouse anti V5 Ab conjugated with horseradish peroxidase (HRP) at 1:5000, Thermo Fisher Scientific, USA), tdTomato (Rabbit anti RFP, Rockland, 1:2000) and actin (mouse anti-actin, Chemicon, 1:20,000) overnight at 4 °C. Next day the blot was washed three times with TBST and incubated with secondary antibodies, goat anti-rabbit (Li-COR) and goat anti-mouse (Li-COR) both at 1:10000. Blots were quantified using Li-COR Odyssey Scanner and software. HRP conjugated primary antibody for V5 tag was detected by chemiluminescence using peroxide and luminol solution (Thermoscientific, USA) and images were captured by measuring chemiluminescence using the AI600 Chemiluminescent Imager (Amersham).

In utero Electroporation

The procedure was performed as described previously [25]. In short, pregnant FvB/NHsD mice at E14.5 of gestation were anesthetized, and the uterus was exposed. The DNA construct (1.5-3 µg/µl) was diluted in fast green (0.05%) and injected in the lateral ventricles of the embryos while still in the uterus, using a glass pipette controlled by a Picospritzer®III device. To ensure the proper electroporation of the injected DNA constructs (1–2 µl) into the progenitor cells, five electrical square pulses of 45 V with a duration of 50-ms per pulse and 150-ms inter-pulse interval were delivered using tweezer-type electrodes connected to a pulse generator (ECM 830, BTX Harvard Apparatus). The electrodes were placed in such a way that the positive pole was targeting the developing somatosensory cortex. Control vector and all four shRNA constructs (3 ug/ul) were mixed separately with 0.05% fast green (Sigma-Aldrich, UK). DNA, consisting of four shRNAs against *Agpat3* gene along with the *tdTomato* expressing plasmid, was injected in three mouse embryos to knock down *Agpat3* in the brain of developing mice. Similarly, a group of three mouse embryos were injected with control shRNA and a *tdTomato* reporter plasmid. The pups were sacrificed after birth at P1 for further immunohistochemistry study.

Immunohistochemistry

At P1 the pups were anesthetized and perfused transcardially with 4% paraformaldehyde (PFA). Brains were removed and fixed in 4% PFA which were then embedded in gelatin and cryoprotected in 30% sucrose using 0.1 M phosphate buffer, frozen on dry ice, and sectioned using a freezing microtome (40–50 µm thick). The coronal sections were washed in 0.1 M phosphate buffer and stained with DAPI (1:10,000, Invitrogen). Selected sections were mounted on glass slides with Mowiol mounting medium (Sigma-Aldrich). Images of the coronal sections were acquired on a confocal microscope (LSM700 Zeiss) using 20x objective for targeted area and on 10x objective for overview images by tile scan imaging.

Neuronal migration and data analysis

Neuronal migration was assessed by selecting three different regions of coronal sections of three different pups for each plasmid on a confocal microscope. A total of nine cortical images of three pups injected with control shRNA and nine cortical images from three pups with *Agpat3* shRNA were analysed. The images were rotated to place cortical layers in the correct position (top layer towards upper side of image) and the number of targeted cells in different layers of somatosensory cortex were counted using ImageJ software. The number and position of cells in each region of interest (ROI) was determined.

For analysis, cortical areas from the pia to the ventricle were divided in 10 equal-sized bins and the percentage of *tdTomato* positive cells per bin was calculated. Sum of the first four bins correspond to the outer layers of (II/III layers) somatosensory cortex [26]. Two tailed unpaired *t* test was used to analyse the number of targeted cells in these bins in three replicates of the knock down group as compared to the control group.

RESULTS

Clinical diagnosis

Five family members presented with severe intellectual disability (ID) and retinitis pigmentosa (IDRP) (Fig. 1a). Four affected individuals (V-1, V-2, V-3 and V-5) participated in this study and had severe ID and variable levels of vision loss (Table 1). Their liver and renal function tests were within normal ranges and the morphology of blood cells on the peripheral blood smear was also normal. All four affected individuals (V-1, V-2, V-3, and V-5) experienced visual problems at night during early childhood, which progressed with age and resulted in complete loss of night vision at ~10 years of age. The cranial computed tomographic (CT) scan of V-5, performed 5 years before MRI, did not reveal any visible brain dysmorphology except the presence of a diffuse thick calvarium (Fig. 1d). MRI testing of V-I at 26 years (Fig. 1e) and his brother V-5 at 18 years of age (Fig. 1f) showed normal features. These affected members had cataract and photophobia since

Table 1. Clinical features of affected members of the family.

Phenotypic and clinical features	V-1	V-2	V-3	V-5
Gender	M	M	F	M
Age at sampling (years)	23	8	21	15
Age at last examination (years)	31	16	29	23
Onset of Visual problem	3 years	18 months	4 years	5 years
Night Blindness	Yes	Yes	Yes	Yes
Bilateral Retinitis pigmentosa (RP)	Yes	Yes	Yes	Yes
Optical Coherence Tomography	No	No	No	Yes
Developmental delay	Yes	Yes	Yes	Yes
Intellectual Disability	Severe	Severe	Severe	Severe
Language/speech delay	Few sentences	Few sentences	Few sentences	Few sentences
Behavior	Aggressive	Aggressive	Aggressive	Aggressive
Fitz	No	Yes	No	No
Social Coordination	Poor	Poor	Poor	Poor
CT Scan	Normal	N/A[a]	N/A	N/A
MRI	Normal	N/A	N/A	Normal
LFTs	Normal	Normal	Normal	Normal
RFTs	Normal	Normal	Normal	Normal
Complete Blood Picture	Normal	Normal	Normal	Normal

[a]N/A: not available.

early childhood, which hindered detailed ophthalmological evaluations. However, direct fundus examination of V-5, the youngest member of the family, at 13 years of age by a local ophthalmologist revealed features compatible with retinitis pigmentosa. This individual has cataract in the left eye, but OCT examination of the right eye at the age of 23 showed poor retinal architecture (Fig. 1g, h). Retina of this male patient (V-5) appears thinned and without clear outer segments (Fig. 1g, h). The one affected female member V-3 was also presented with amenorrhea, whereas all affected male individuals did not experience nocturnal emission since adulthood. All affected individuals lacked the concept of self-care and both qualitative and quantitative skills, exhibited aggressive fighting behavior, and dependency on others for routine activities. They also exhibited ambulation and speech delays and could only speak short sentences. None of the affected individuals have attended formal or special education schools. Overall assessment of members of this family showed severe ID with IQ scores between 20 to 30. The clinical information of this family was unique and did not show any similarity with any previously reported syndromes, therefore we characterized this condition as intellectual disability retinitis pigmentosa (IDRP) syndrome.

Homozygosity mapping and exome sequencing

Homozygosity mapping using whole genome genotype data obtained from three affected (V-2, V-3, V-5) and three normal (III-3, V-4, V-6) family members revealed peaks on chromosome 3, 4, 5, 7, 8, 18 and 21 (Fig. 1b). But further analysis of the genotype data of each region showed the presence of homozygosity in the healthy family members as well. Further filtering of the identified homozygous genomic regions, based on haploidentity, led to the identification of a common homozygous region of 5.65 Mb (chr 21: 40103951– 45755360; hg19) on chromosome 21 (Fig. 1b). Three affected (V-2, V-3, V-5) individuals were homozygous for this genomic region, but healthy individuals (III-3, V-4, V-6) were heterozygous.

Exome sequencing of affected individual V-3 identified thousands of variants but further filtering revealed 23 rare and potentially damaging homozygous variants (Supplementary Table 1). Only the variants identified in *AGPAT3* and *PWP2* were present within the 5.65 Mb homozygous region mapped on chromosome 21 but *AGPAT3* was selected as a candidate gene for IDRP syndrome. A missense variant c.2606 A > C (p.Asn869Thr) was found in exon 21 of *PWP2* (NM_005049) but pathogenicity of the variant was predicted to be tolerant and benign by various *in-silico* tools like SIFT, Polyphen2, FATHMM. The variant also has a very small CADD score (0.95) thus this variant is considered as nondamaging and excluded from further analysis. The nonsense variant c.747 C > A (GRCh37/hg19) (p.Tyr249Ter) is present in exon 7 of *AGPAT3* (NM_020132) (Fig. 2) and is predicted to be deleterious or damaging by *in-silico* tools, and is absent in dbSNP (Build 132). The nonsense variant is also absent from gnomAD database v2.1.1. The CADD score for c.747 C > A variant is 35. Sanger Sequencing confirmed that variant (c.747 C > A) co-segregates with the disease phenotype (Fig. 1c) i.e., affected family members are homozygous and unaffected members either heterozygous or homozygous wildtype. The variant affects six major *AGPAT3* transcript isoforms possibly by activating the nonsense mediated decay (NMD). Alternatively, since the nonsense variant is situated before the second transmembrane region and the putative C-terminal ER retention motif, a truncated AGPAT3 protein would not be expected to yield a functional protein [19].

Considering the presence of IDRP syndrome in this family, we carefully analysed the exome data and BAM file of individual V-3 to exclude the possible involvement of genes known for Bardet Biedl (MIM 209900), Joubert (MIM 213300), and Meckel Gruber (MIM 249000) syndromes. Detailed analysis of all genomic regions, carrying genes for above mentioned syndromes showed minimum coverage/read depth of 12x to aid in assuring that possible pathogenic variants within the coding exons were not excluded during variant calling.

In vitro Effect of Mutant *AGPAT3* (p.Tyr249Ter)

The effect of *AGPAT3* nonsense variant was further explored by heterologous expression in HEK-293T cells. Transfection of HEK-293T cells with N-terminally tagged wild-type or mutant *AGPAT3* (carrying p.Tyr249Ter variant) revealed the absence of AGPAT3

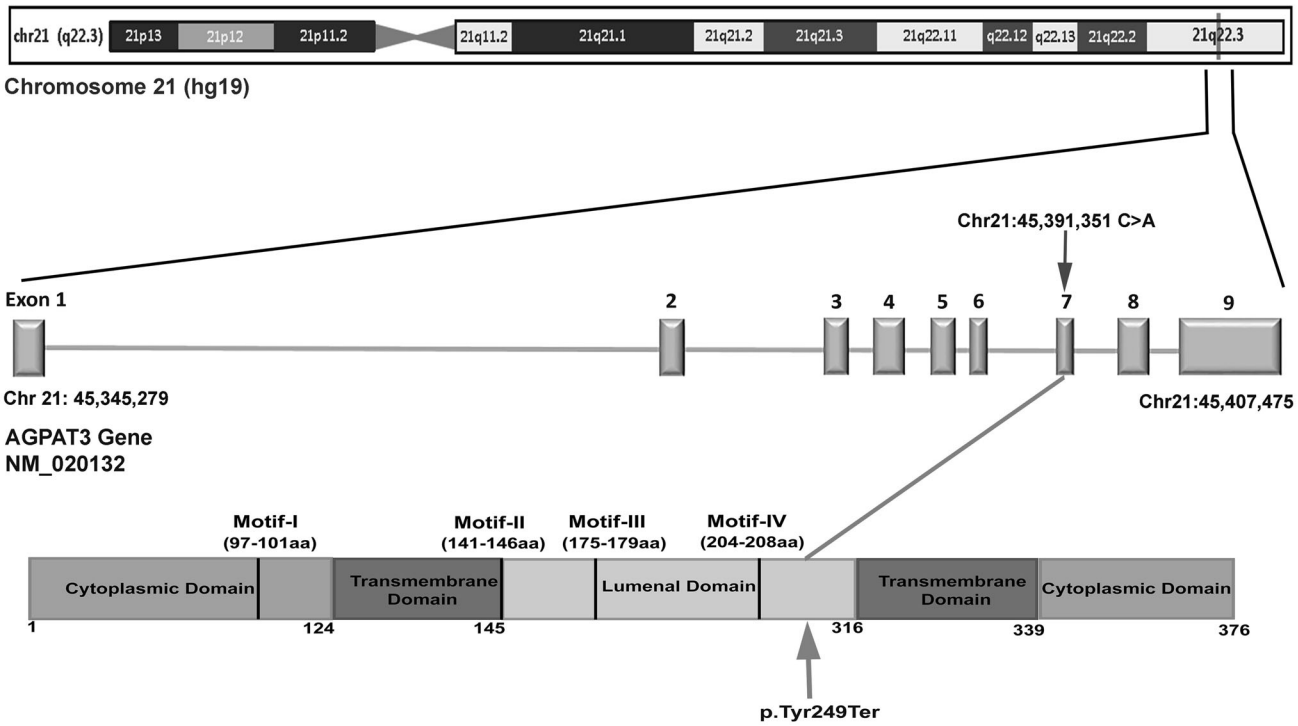

Fig. 2 Map of chromosome 21 showing location of AGPAT3 gene. Schematic representation of gene and protein shows the position of identified variant. Domains and motifs of AGPAT3 protein are also shown.

mutant protein (Fig. 3a, b), likely due to the protein instability. Therefore, it can be proposed that the *AGPAT3* variant results in protein degradation. We speculate that similar loss of functional protein in affected individuals of family MR23 might be responsible for IDRP syndrome.

Knock down of *AGPAT3* impairs neuronal migration in vivo

AGPAT3 is expressed in all human and mice brain tissues except corpus callosum (https://www.proteinatlas.org/ENSG00000160216-AGPAT3/brain). RNA-seq analysis, from human protein atlas database, shows that retina as well as brain are both amongst the highest *AGPAT3* mRNA expressing tissues in humans (https://www.proteinatlas.org/ENSG00000160216-AGPAT3/summary/rna). To evaluate the effect of *AGPAT3* loss of function mutation on neuronal function, we made use of the neuronal migration assay. Neuronal migration is a highly intricate process in cortical development and very sensitive to neuronal dysfunction. This neuronal migration assay measures the ability of targeted neural cells in the ventricular zone to successfully migrate to layer 2/3 of the somatosensory cortex [27]. The *Agpat3* gene was knocked down by injecting shRNA through *in utero* electroporation in mice at day E14.5. The effect of *Agpat3* knockdown on neuronal positioning was studied at P1. Brain sections with cells expressing a control vector showed a normal migration pattern of neurons, with the majority of the neurons reaching layer II/III of the somatosensory cortex (Fig. 3c). However, sections from mice injected with shRNA directed against *Agpat3* showed reduced migration of neurons from subventricular zone to somatosensory cortex (Fig. 3d). There was a significant difference in the percentage of the transfected cells in bins 1-4 which corresponded to the upper three layers of the cortex (Fig. 3e). A substantial number of *Agpat3* shRNA targeted cells were localized in the intermediate zone compared to cells transfected with a control vector (Fig. 3e).

We further assessed the effect of *Agpat3* knock down on neuronal positioning in the upper three cortical layers (by considering the first 4 bins out of 10 bins representing all the cortical layers) and found that 86.55 % of transfected cells were present in the upper three cortical layers in the control (Fig. 3f). In the case of *Agpat3* knock down, neuronal migration to the first three cortical layers was significantly reduced (Fig. 3f) as only 45.27% transfected cells were present within these layers. Taken together, this suggest that reduced AGPAT3 levels results in impaired neuronal functioning.

DISCUSSION

In this study, we describe a novel nonsense variant in *AGPAT3* in a family presenting with severe ID and RP. We showed that a nonsense variant in *AGPAT3* results in the loss of function, likely due to protein instability. Initially, involvement of JS was considered in this family due to the presence of ID and RP, but absence of molar tooth sign, a radiologic finding that includes cerebellar vermis hypoplasia and malformation of the brainstem, in MRI images of two patients of this family ruled out the involvement of JS [28]. Similarly, detailed clinical and laboratory findings helped to exclude BBS, SLS, CS, and MKS. Therefore, here we report on a family with four affected members that have a new syndrome, IDRP.

AGPAT3 consists of 9 exons and its encoded protein works as an enzyme which is also known as lysophosphatidic acid acyltransferase 3 (LPAAT3). This enzyme (EC:2.3.1.51) belongs to the family of AGPAT (1-acyl-sn-glycerol 3-phosphate acyltransferase) enzymes which catalyzes the conversion of lysophosphatidic acid (LPA) to phosphatidic acid (PA) [17]. AGPAT3 is a transmembrane protein, consisting of four motifs (I-IV) present in cytoplasmic, luminal and transmembrane domains, and is localized to the golgi complex and ER [19]. Studies have shown that these motifs are important for catalysis and substrate binding [19, 20]. Since the nonsense variant identified in our family is expected to result in early termination of the protein, the mutant mRNA in patients likely undergoes nonsense-mediated decay [29], but unfortunately patient derived samples were not available to validate this

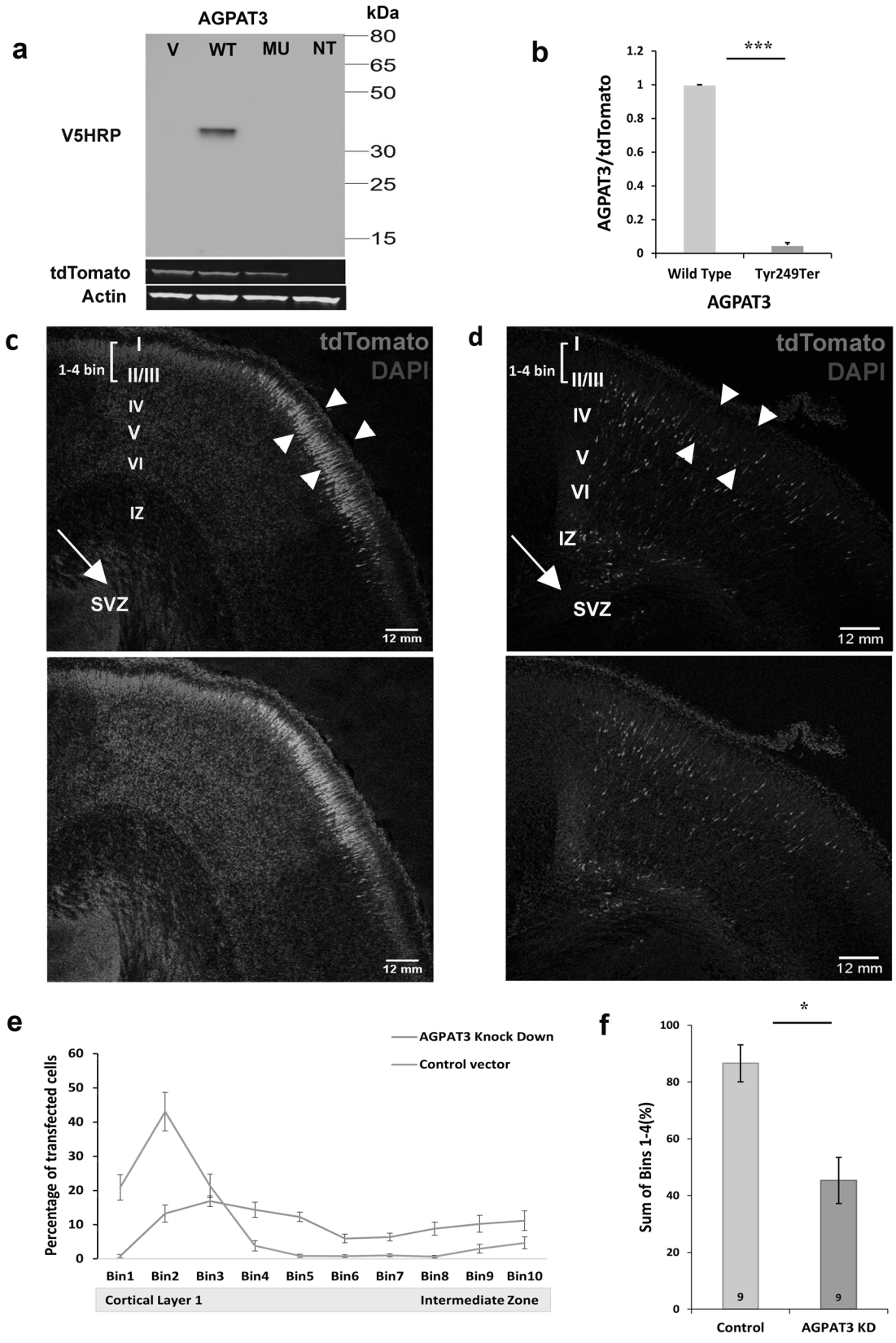

assumption. HEK-293T cell-based analysis confirmed the presence of overexpressed wild type protein, but the mutant AGPAT3 protein was absent (Fig. 3a, b) indicating the instability of the truncated protein. Therefore, it is expected that loss of function of *AGPAT3* probably disrupts the conversion of LPA to PA and this may alter membrane morphology [18].

According to Human Protein Atlas, *AGPAT3* expression is highest in the brain but an earlier study also detected expression

Fig. 3 AGPAT3 overexpression and knockdown. a Western blot of HEK293T cells (triplicate) transfected with vector (V), V5-tagged WT AGPAT3, V5-tagged mutant AGPAT3 Tyr249Ter (MU) and non-transfected (NT) samples. Antibodies against tdTomato, B-actin and V5 were used. **b** Quantification of Western blot (a) showing relative V5-AGPAT3 WT and mutant expression levels, normalized to tdTomato using two-tailed unpaired *t* test ($p = 2.58 \times 10^{-8}$). **c** Images of in utero Electroporation (IUE), transfected with control vector and (**d**) Agpat3 shRNA in merged (upper) and black and white (lower) panels. Red color (tdTomato) indicates transfected cells and blue (DAPI) DNA-staining showing the general cortical structure. Arrow heads indicate II/III somatosensory cortical layers, and the arrow represents the subventricular zone (SVZ). Quantification of neuronal migration: **e** Percentage of neuronal cells migrated from intermediate zone (Bin10) to cortical layer 1 (Bin1) in mouse brain coronal sections ($n = 3$). **f** Statistical analysis of the percentage of cells in bins 1-4 corresponding to layers II/III of somatosensory cortex using two-tailed unpaired *t* test ($p = 1.6 \times 10^{-2}$), numbers in the graph bar represent the number of analyzed pictures where $n = 3$.

in the mouse retina [21]. They further observed a progressive increase of *AGPAT3* expression in the retina in an age-dependent manner [21]. This study extended the role of *AGPAT3* beyond the regulation of golgi trafficking [18] and provided data to support its role in the structural maintenance of membranes. Docosahexaenoic acid (DHA), a polyunsaturated fatty acid, is essential for the organization of discs in retinal photoreceptor cells and it is frequently present in phospholipids (PL) thus labeled as PL-DHA. PL-DHA is synthesized by AGPAT3 enzyme and knockdown of this enzyme in mice results in the disappearance of PL-DHA from the outer segments of the photoreceptor cells [21]. PL-DHA is important for disc morphology and visual function of photoreceptors and *Agpat3* knockout mice demonstrated abnormal photoreceptor disc orientation and visual function [21]. Young *Agpat3* knockout mice (2 weeks old) have normal photoreceptors compared to older mice (3-8 weeks old) which have abnormal photoreceptors, especially in the outer segment. Affected members of our family also presented progressive vision loss and OCT of a male patient (23-year-old) showed abnormal outer segment. This phenotypic presentation is in line with the phenotype observed in *Agpat3* knockout mice, but this male patient (V-5) has cataract in the left eye, which was not reported in the mouse model.

AGPAT3 is reported to directly regulate the trafficking events in golgi complex by altering the ratio of phospholipids and lysophospholipids. Phosphatidic acid generated by *AGPAT3* is present at vesicles and induces the negative curvature to ensure the proper fission of the membrane vesicles [19, 30]. The absence of both allelic products of *AGPAT3* in patients with homozygous mutations, probably changes the ratio of LPA to PA and thus alters golgi morphology and membrane trafficking by changing the positive or negative curvature leading to fragmentation of golgi cisternae [18]. This is further supported by another study on *Agpat3* knockout mice which exhibited male infertility [22]. Interestingly, *Agpat3* knockout mice have a reduced sperm count, but infertility was due to morphological abnormalities of sperm which delayed their release. It is hypothesized that abnormal photoreceptor disc morphology and sperm abnormalities, observed in *Agpat3* knockout mice, are probably caused by the altered LPA to PA ratio, but additional studies are required to establish the exact mechanism. We also observed features in affected members of MR23 family which indicate probable involvement of infertility (i.e., all affected males lacked nocturnal emissions and the one affected female presented with amenorrhea), but this could not be investigated further. It is important to note that infertility is only reported in male knockout mice, but female patient (V-3) presenting with amenorrhea may indicate the possible involvement of female infertility as well.

Prior studies on *Agpat3* knockout mice focused on retina and sperm, but no information is available regarding its role in the brain. In our study, knock down of *Agpat3* in mouse brains showed a deficit in neuronal migration to the outer layers of somatosensory cortex, indicating that *Agpat3* knock down impaired neuronal functioning. Notably, such a delay in the IUE assay does typically not mean that patients are likely to present with cortical migration deficits. For instance, functional studies on variants identified in *CAMK2A,CAMK2B or TAOK1* gene affected neuronal migration while the majority of the patients representing these mutations had normal MRI scans [26]. Hence the migration delay appears to be the result of gene knock-down in sparsely targeted cells that have to compete with non-targeted cells. In addition, the migration delay in mice observed at P1, is often just a temporary delay that is resolved within a few weeks.

We identified a family with intellectual disability retinitis pigmentosa (IDRP) syndrome caused by a nonsense variant in *AGPAT3* gene. We found that nonsense mutation renders the protein unstable and knock down of *Agpat3* in mouse brains highlights its importance in neuronal functioning. Since no other cases are present in the literature suggesting *AGPAT3* involvement in IDRP syndrome, therefore further cases should confirm the role of *AGPAT3* in neurological diseases. Moreover, studies are also required to explore the detailed function of *AGPAT3* in syndromic ID.

Web resources

Homozygosity Mapper http://www.homozygositymapper.org/
wANNOVAR http://wannovar.wglab.org/
Human Protein Atlas database https://www.proteinatlas.org/
1000 Genomes Browser https://www.internationalgenome.org/
gnomAD Browser https://gnomad.broadinstitute.org/

DATA AVAILABILITY

Data generated during the study are available from corresponding author on reasonable request. The variant information has been deposited in Clinvar with submission ID SCV 003929458.

REFERENCES

1. Bee YM, Chawla M, Zhao Y. Whole exome sequencing identifies a novel and a recurrent mutation in BBS2 gene in a family with Bardet-Biedl syndrome. BioMed Res Int. 2015;2015:524754.
2. Novas R, Cardenas-Rodriguez M, Irigoín F, Badano JL. Bardet-Biedl syndrome: Is it only cilia dysfunction? FEBS Lett. 2015;589:3479–91.
3. Usta M, Urganci N, Özçelik G, Çetinçelik Ü, Kafadar I, Özgüven BY. Joubert syndrome and related disorders: a rare cause of intrahepatic portal hypertension in childhood. Eur Rev Med Pharmacol Sci. 2015;19:2297–300.
4. Cohen MM Jr, Hall BD, Smith DW, Graham CB, Lampert KJ. A new syndrome with hypotonia, obesity, mental deficiency, and facial, oral, ocular, and limb anomalies. J Pediatr. 1973;83:280–4.
5. Ronquillo CC, Bernstein PS, Baehr W. Senior-Løken syndrome: a syndromic form of retinal dystrophy associated with nephronophthisis. Vis Res. 2012;75:88–97.
6. Smith UM, Consugar M, Tee LJ, McKee BM, Maina EN, Whelan S, et al. The transmembrane protein meckelin (MKS3) is mutated in Meckel-Gruber syndrome and the wpk rat. Nat Genet. 2006;38:191–6.
7. Yang XR, Benson MD, MacDonald IM, Innes AM. A diagnostic approach to syndromic retinal dystrophies with intellectual disability. Am J Med Genet Part C, Semin Med Genet. 2020;184:538–70.
8. Tatour Y, Sanchez-Navarro I, Chervinsky E, Hakonarson H, Gawi H, Tahsin-Swafiri S, et al. Mutations in SCAPER cause autosomal recessive retinitis pigmentosa with intellectual disability. J Med Genet. 2017;54:698–704.
9. Fasham J, Arno G, Lin S, Xu M, Carss KJ, Hull S, et al. Delineating the expanding phenotype associated with SCAPER gene mutation. Am J Med Genet Part A. 2019;179:1665–71.
10. Wormser O, Gradstein L, Yogev Y, Perez Y, Kadir R, Goliand I, et al. SCAPER localizes to primary cilia and its mutation affects cilia length, causing Bardet-Biedl syndrome. Eur J Hum Genet : EJHG. 2019;27:928–40.

11. Coppieters F, Ascari G, Dannhausen K, Nikopoulos K, Peelman F, Karlstetter M, et al. Isolated and syndromic retinal dystrophy caused by biallelic mutations in RCBTB1, a gene implicated in ubiquitination. Am J Hum Genet. 2016;99:470–80.
12. Di Donato N, Neuhann T, Kahlert AK, Klink B, Hackmann K, Neuhann I, et al. Mutations in EXOSC2 are associated with a novel syndrome characterised by retinitis pigmentosa, progressive hearing loss, premature ageing, short stature, mild intellectual disability and distinctive gestalt. J Med Genet. 2016;53:419–25.
13. Shimizu T. Lipid mediators in health and disease: enzymes and receptors as therapeutic targets for the regulation of immunity and inflammation. Annu Rev Pharmacol Toxicol. 2009;49:123–50.
14. van Meer G, Voelker DR, Feigenson GW. Membrane lipids: where they are and how they behave. Nat Rev Mol cell Biol. 2008;9:112–24.
15. Yamashita A, Hayashi Y, Nemoto-Sasaki Y, Ito M, Oka S, Tanikawa T, et al. Acyltransferases and transacylases that determine the fatty acid composition of glycerolipids and the metabolism of bioactive lipid mediators in mammalian cells and model organisms. Prog lipid Res. 2014;53:18–81.
16. Agarwal AK. Lysophospholipid acyltransferases: 1-acylglycerol-3-phosphate o-acyltransferases. from discovery to disease. Curr Opin Lipidol. 2012;23:290–302.
17. Prasad SS, Garg A, Agarwal AK. Enzymatic activities of the human AGPAT isoform 3 and isoform 5: localization of AGPAT5 to mitochondria. J lipid Res. 2011;52:451–62.
18. Schmidt JA, Brown WJ. Lysophosphatidic acid acyltransferase 3 regulates Golgi complex structure and function. J cell Biol. 2009;186:211–8.
19. Schmidt JA, Yvone GM, Brown WJ. Membrane topology of human AGPAT3 (LPAAT3). Biochem Biophys Res Commun. 2010;397:661–7.
20. Yamashita A, Nakanishi H, Suzuki H, Kamata R, Tanaka K, Waku K, et al. Topology of acyltransferase motifs and substrate specificity and accessibility in 1-acyl-sn-glycero-3-phosphate acyltransferase 1. Biochim et Biophys Acta. 2007;1771:1202–15.
21. Shindou H, Koso H, Sasaki J, Nakanishi H, Sagara H, Nakagawa KM, et al. Docosahexaenoic acid preserves visual function by maintaining correct disc morphology in retinal photoreceptor cells. J Biol Chem. 2017;292:12054–64.
22. Iizuka-Hishikawa Y, Hishikawa D, Sasaki J, Takubo K, Goto M, Nagata K, et al. Lysophosphatidic acid acyltransferase 3 tunes the membrane status of germ cells by incorporating docosahexaenoic acid during spermatogenesis. J Biol Chem. 2017;292:12065–76.
23. Seelow D, Schuelke M, Hildebrandt F, Nürnberg P. HomozygosityMapper-an interactive approach to homozygosity mapping. Nucleic Acids Res. 2009;37:W593–9. Web Server issue
24. Ansar M, Santos-Cortez RL, Saqib MA, Zulfiqar F, Lee K, Ashraf NM, et al. Mutation of ATF6 causes autosomal recessive achromatopsia. Hum Genet. 2015;134:941–50.
25. Proietti Onori M, Koopal B, Everman DB, Worthington JD, Jones JR, Ploeg MA, et al. The intellectual disability-associated CAMK2G p.Arg292Pro mutation acts as a pathogenic gain-of-function. Hum Mutat. 2018;39:2008–24.
26. Küry S, van Woerden GM, Besnard T, Proietti Onori M, Latypova X, Towne MC, et al. De novo mutations in protein kinase genes CAMK2A and CAMK2B cause intellectual disability. Am J Hum Genet. 2017;101:768–88.
27. Tabata H, Nakajima K. Efficient in utero gene transfer system to the developing mouse brain using electroporation: visualization of neuronal migration in the developing cortex. Neuroscience. 2001;103:865–72.
28. Parisi MA, Doherty D, Chance PF, Glass IA. Joubert syndrome (and related disorders) (OMIM 213300). Eur J Hum Genet. 2007;15:511–21.
29. Hentze MW, Kulozik AE. A perfect message: RNA surveillance and nonsense-mediated decay. Cell. 1999;96:307–10.
30. Kooijman EE, Chupin V, de Kruijff B, Burger KN. Modulation of membrane curvature by phosphatidic acid and lysophosphatidic acid. Traffic (Cph, Den). 2003;4:162–74.

ACKNOWLEDGEMENTS

We acknowledge the volunteer participation of patients and other members of the family. We are thankful to the Higher Education Commission of Pakistan for providing International Research Support Fellowship to Madiha Amin Malik. Deborah A Nickerson made significant contributions to the work. Dr. Nickerson was a very distinguished and highly respected researcher who passed away too early. Therefore, we acknowledge her work and the impact that she and her research activities are still making. We are also thankful to University of Washington Center for Mendelian Genomics for their support in the exome sequencing.

AUTHOR CONTRIBUTIONS

Conceptualization and study design: MAM, YE, SML, MA; Family recruitment and clinical tests: MANS; Homozygosity mapping (HB) and exome sequencing (ES): AA, IS, MJB, RLPS-C; HB and ES data analysis: MAM, MANS, AA, RLPS-C; AGPAT3 constructs and western blotting (WB) experiments and data analysis: MAM, EM; In utero electroporation (IUE) experiments: MAM, IW; IUE data analysis: MAM; First draft of manuscript: MAM, IS, SML, MA: Manuscript review and editing: MAM, EM, MRA, YE, SML, MA. All co-authors read and approved the manuscript.

FUNDING

The research was supported by National Research Grant (NRPU-7099) to Muhammad Ansar by Higher Education Commission of Pakistan, International Research Support Fellowship (IRSIP) to Madiha Amin Malik by Higher Education Commission of Pakistan and by the National Institute of Health – National Institute of Child Health and Development grant R01 HD109342 to Suzanne M. Leal.

COMPETING INTERESTS

The authors declare no competing interests.

ETHICAL APPROVAL

It is certified that the study was performed in accordance with the ethical standards of 1964 Helsinki Declaration. The study was conducted by obtaining ethical approval from Bio-Ethics Committee (BEC-562) of Faculty of Biological Sciences, Quaid-I-Azam University, Islamabad, Pakistan and Institutional Review Board (IRB), at Columbia University (IRB-AAAS3433), USA. Animal experiments were performed in accordance with European Commission Council Directive 2010/63/EU (CCD approval AVD101002017893) at Erasmus Medical Center, Rotterdam, Netherlands.

ADDITIONAL INFORMATION

Supplementary information The online version contains supplementary material available at https://doi.org/10.1038/s41431-023-01475-w.

Correspondence and requests for materials should be addressed to Suzanne M. Leal or Muhammad Ansar.

Reprints and permission information is available at http://www.nature.com/reprints

Publisher's note Springer Nature remains neutral with regard to jurisdictional claims in published maps and institutional affiliations.